A COMPARATIVE STUDY OF PHOTOCONDUCTIVITY DECAY IN GRANULAR AND NANOWIRE ZnO

Vitalie Postolache

National Center for Materials Study and Testing, Technical University of Moldova,
Bd. Stefan cel Mare 168, Chisinau, MD-2004 Republic of Moldova
E-mail: postolache_vitalie@yahoo.com

(Received January 19, 2016)

Abstract

A comparative analysis of transient photoconductivity in microgranular ZnO and ZnO nanowires prepared by oxidizing bulk ZnTe and ZnTe nanowires, respectively, is performed in this paper. The measurements are carried out at different temperatures in microgranular ZnO and at room temperature in the ambient air in ZnO nanowire networks. The mechanisms of photoconductivity decay are discussed taking into account the morphological features of the samples and the range of measured relaxation times.

1. Introduction

Long-duration-photoconductivity decay and persistent photoconductivity (PPC) inherent in many materials can have a significant effect on the characteristics of device structures prepared on their basis, such as UV detectors, field effect transistors, gas sensors, etc. in terms of their sensitivity, noise properties, dark level, and response speed. Different mechanisms were considered as the origin of PPC. The origin of PPC in moderately doped bulk semiconductors, such as III–V alloys, is believed to be related to atomic defect centers with unusual properties, such as defects with bistable character [1, 2], AX [3], or DX centers [4–7]. AX centers are acceptors, while DX centers are donors.

It is generally accepted that the mechanism leading to the metastable behavior of DX centers is due to the large lattice relaxation following electron capture by the DX state. It is also generally believed that the DX center should behave as the so-called negative-U center [8–10].

In highly doped compensated semiconductors, it was suggested that the microscopic inhomogeneity caused by impurity distribution is the most probable cause of the PPC phenomenon [11–15]. According to this model, the spatial separation of the photogenerated electrons and holes by macroscopic potential barriers occurs due to band bending around doping inhomogeneities; however, these potential barriers can also be formed at planar surfaces, interfaces, junctions, etc. If these potential barriers are sufficiently high in comparison with the thermal voltage kT/q, the lifetime of the electron and hole becomes very long. This mechanism with macroscopic potential barriers was also applied to explain the PPC in II–VI semiconductor alloys [16–19]. It was suggested that, in this case, the spatial separation between stored charge carriers by random local-potential fluctuations is caused by compositional fluctuations.

The origin of PPC and optical quenching of photoconductivity (PC) were also

investigated in bulk GaN layers. It was demonstrated to originate from metastable defects and explained in terms of a model combining two previously proposed schemes with electron traps playing the main role in PPC and hole traps inducing optical quenching of PC [20, 21].

Long-duration-photoconductivity decay and PPC have also been shown to be inherent in porous materials [22, 23]. Similarly to highly doped compensated semiconductors and alloys with compositional fluctuations, PPC in porous materials was suggested to be caused by potential barriers induced by random local-potential fluctuations; however, in this case, the potential fluctuations are caused by porosity.

The PPC in nanowires, for instance, ZnO and GaN nanowires characterized by a high surface-to-volume ratio, has a different nature. It is generally believed that, in this case, PPC is caused by a strong surface band bending (SBB) effect instead of a bulk trap effect [24, 25]. The significant SBB in nanowires localizes the excess carriers. As a result, strongly reduced recombination of holes with those electrons trapped at the surface considerably extends the carrier lifetime. It was shown that SBB in ZnO nanowires is strongly governed by surface adsorbed species, among which oxygen molecules play a major role [26–29]. In general, surface-induced carrier localization is proposed to be one of the main causes of PPC in nanostructures with a high surface-to-volume ratio, such as utrathin InP membranes and nanoperforated GaN membranes [30, 31].

Regardless of the nature of PPC, these phenomena can have a significant effect on the characteristics of device structures, such as UV detectors, field effect transistors, gas sensors, etc. in terms of their sensitivity, noise properties, dark level, and response speed.

The goal of this paper is to perform a comparative study of PC decay in microgranular ZnO structures and nanowires with reference to the mechanism governing the PC relaxation processes.

2. Sample preparation technique

Nanostructured ZnO samples were prepared on the basis of Na-doped bulk ZnTe single crystals with a free hole concentration of 3×10^{18} cm^{-3}. Microgranular ZnO and ZnO nanowires were prepared by two different technological routes. ZnTe bulk crystals were annealed in a temperature interval of 300 to 800 ^{o}C in air for 1 h to produce granular ZnO. The sizes of granules can be varied by changing the annealing temperature. The morphology of a granular ZnO sample with mean granule dimensions of around 1 μm obtained after thermal treatment at 700^{o}C is shown in Fig. 1a. X-ray diffraction and photoluminescence analyses demonstrated that annealing at 700^{o}C leads to a total transformation of the initial ZnTe crystals into wurzite ZnO [32], the photoluminescence spectra being dominated by the emission related to the recombination of donor bound D^0X excitons. According to the second technological route, a template of ZnTe nanowires with a mean diameter around 50 nm is produced in the first step by electrochemical treatment of ZnTe crystals as described elsewhere [32]. Anodic etching was conducted in an HNO_3 : HCl : H_2O electrolyte at a ratio of 5 : 20 : 100 at 25^{o}C with the application of 0.3-s voltage pulses at a frequency of 1 Hz and an amplitude of 5 V. The ZnTe nanowires are transformed into ZnO nanowires in the second step by thermal treatment. The morphology of the nanowires does not change during annealing at 500^{o}C (Fig. 1b), while the material is totally oxidized. The morphology and chemical composition microanalyses of the samples were conducted using a VEGA TESCAN TS 5130MM scanning electron microscope equipped with an Oxford Instruments INCA energy dispersive X-ray system.

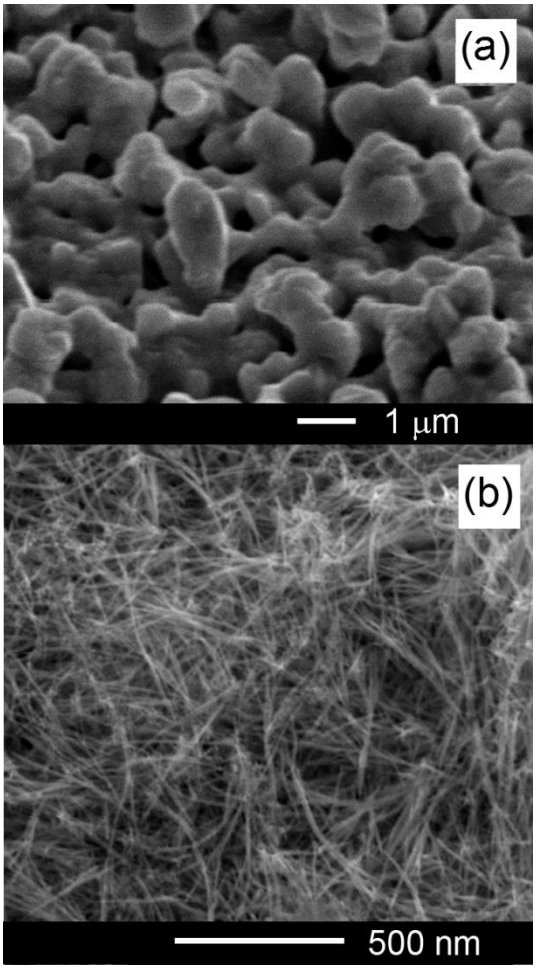

Fig. 1. Morphology of the ZnO microgranular material prepared by thermal treatment of bulk ZnTe crystals (a) and ZnO nanowires prepared from ZnTe nanowires (b).

3. Experimental details of measuring PC decay

The electrical contacts to samples for measuring PC were prepared using a conductive silver paste. Since the decay time is long enough in a network of ZnO nanowires, a 366-nm excitation beam of an Hg arc lamp was mechanically shut in the PC relaxation experiments. The experiments were performed at room temperature in ambient air.

The photoresponse from granular samples was measured with the set-up schematically shown in Fig. 2. The UV illumination was provided by a UV light-emitting diode (LED) with a peak wavelength of 370 nm powered by a G6-15 function generator. The sample was biased at 5 V. The signal from a resistor connected in series with the investigated sample was measured by a digital sampling storage C9-8 oscilloscope. The signal from the oscilloscope was introduced in an IBM computer via IEEE-488 interface for further data processing. The sample was mounted in a LTS-22-C-330 Workhorse-type optical cryogenic system to perform measurements in a

temperature interval of 100–300 K.

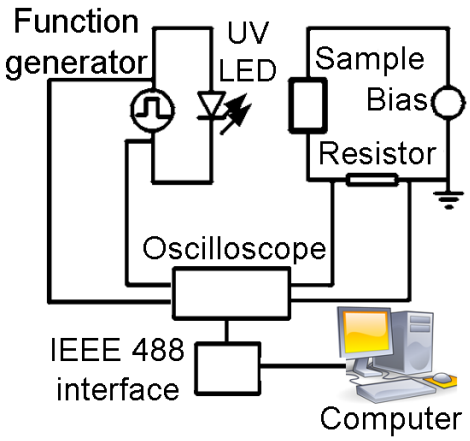

Fig. 2. Schematic diagram of the setup for measuring the PC response from ZnO nanowires.

4. PC relaxation in microgranular ZnO

The excitation square wave from the function generator is illustrated in Fig. 3a; the photoresponse of the microgranular ZnO sample is shown in Fig. 3b. It is evident from Fig. 3b that the PC relaxation is nearly symmetric with respect to PC build-up and decay. The analysis of these relaxation curves shows that the relaxation time decreases from about 200 ms at 100 K to 50 ms at 150 K with a further increase to 300 ms at 230 K. Therefore, a nonmonotonic temperature dependence on the PC relaxation time is observed.

A more detailed dependence of the relaxation time in the Arrhenius plot is presented in Fig. 4. The relaxation time was determined, for each experimental point presented in Fig. 4, from the analysis of the PC decay curve measured at the respective temperature. This relaxation time dependence resembles a typical behavior of the carrier lifetime for carrier recombination via recombination centers. In the case of carrier recombination via recombination centers, the relaxation time is constant and equals τ_p until the Fermi level intersects the defect energy level. Further, the lifetime increases exponentially with temperature up to the region of intrinsic conductivity, with a consequent exponential decrease. However, some important observations are in contradiction with this model of recombination, namely: (i) the relaxation time (~50–300 ms) is significantly higher than the carrier lifetime (~ several μs) typical for processes governed by recombination centers; (ii) there are some contradictions related to the parameters deduced from this model: according to this model, one can estimate the position of the recombination level by determining the temperature of Fermi-level intersection with the defect energy level $T_1 \approx 187$ K, the temperature of the transition to the intrinsic conductivity $T_2 \approx 230$ K, and the intersection of the extrapolated $T_1 \div T_2$ segment (Fig. 4) with the ordinate axis which gives the value of $\ln(\tau_{p0}N_c/n_0) = 8$; by extracting the value of $\ln \tau_{p0} = -3$ from this value, we obtain $\ln(N_c/n_0) = 11$; then, one can calculate the defect energy level $E_c - E_t = kT_1\ln(N_c/n_0) = 177$ meV; the second observation is that the value of T_1 and T_2 are too close to each other for the given defect energy level; (iii) the temperature of transition to intrinsic conductivity $T_2 = 230$ K is unlikely low, while this usually occurs at temperatures much higher than the room temperature in this kind of

samples [33]; (iv) there is an increase of the relaxation time with decreasing temperature from 150 to 100 K.

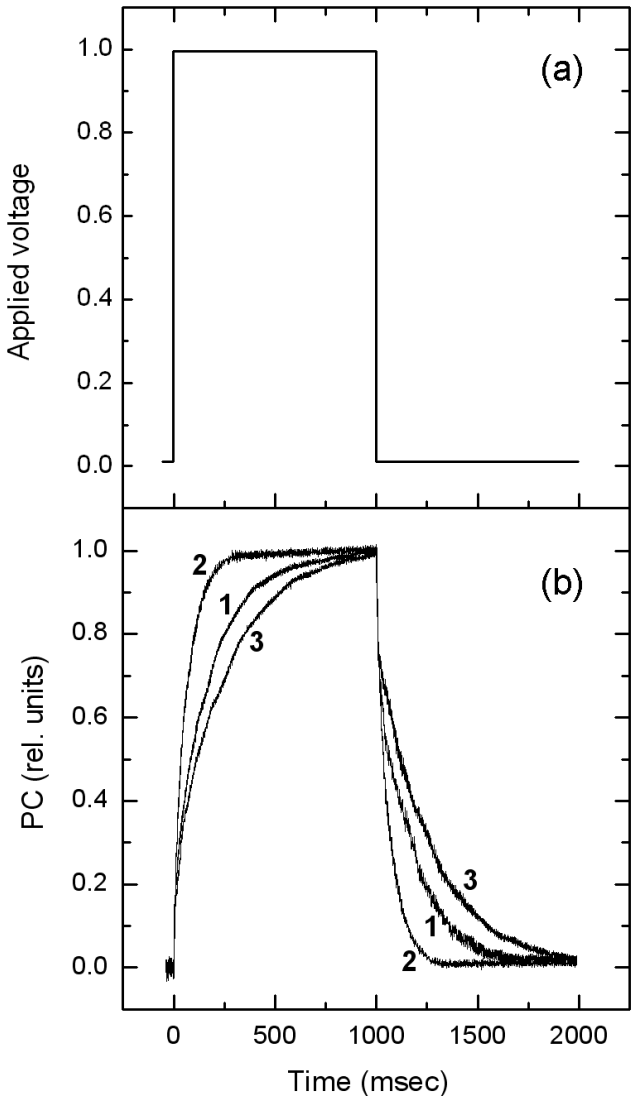

Fig. 3. Excitation pulse (a) and photoconductivity response measured from the microgranular ZnO sample at a temperature of 100 (curve 1), 150 (curve 2), and 230 K (curve 3).

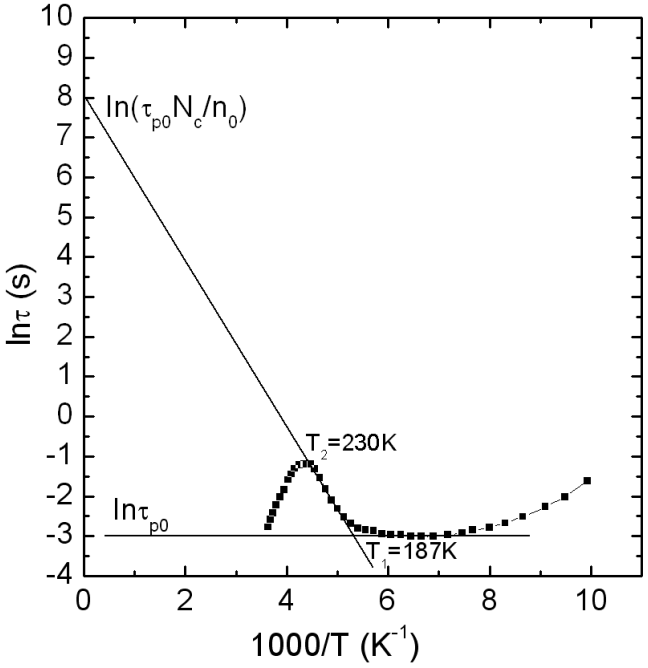

Fig. 4. Temperature dependence of the PC decay time in the microgranular ZnO sample.

The above mentioned observations indicate the implication of traps in the nonequilibrium carrier recombination processes. In the case of trap implication, the effective relaxation time is given by the expression

$$\tau' = \tau_n \left(1 + \frac{M}{N_c} e^{\frac{(E_c - E_M)}{kT}} \right), \tag{1}$$

where τ_n the lifetime of the electron, M is the trap concentration, N_c is the effective density of states in the conduction band, E_c is the energy of the conduction band bottom, and E_M is the position of the trap energy level.

Therefore, one can conclude that the charge transport in microgranular ZnO structures occurs due to percolation (interconnections) of grains and the PC relaxation is governed by bulk processes in the grains with a significant effect from trapping centers.

5. Long-duration PC decay in ZnO nanowires

The PC relaxation processes in nanowire samples has a different nature. Figure 5 shows the PC build-up and decay in a network of ZnO nanowires with the morphology illustrated in Fig. 1b. First of all, the relaxation time is two orders of magnitude longer than that for the microgranular sample. This large relaxation time cannot be explained by trapping effects of bulk centers. Models with microscopic (atomic) energy barriers at centers with large lattice relaxation, such as DX centers, have not been reported in ZnO either. On the other hand, the SBB effects are generally accepted as the origin for long relaxation times and PPC in ZnO nanowires [25–29].

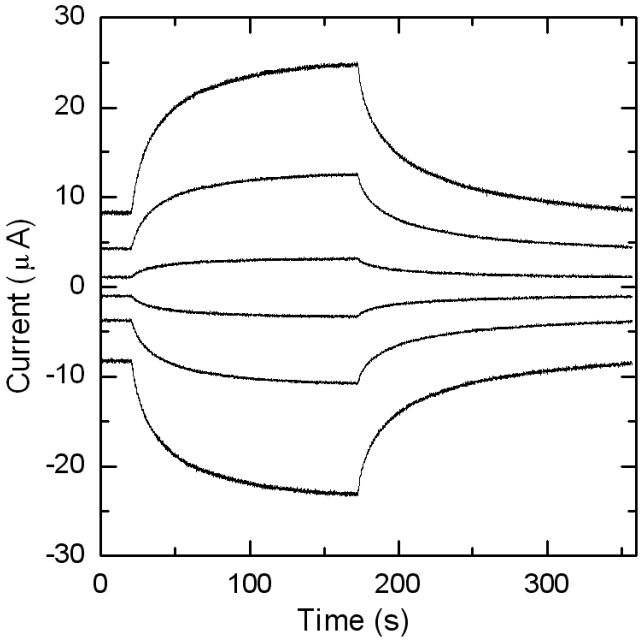

Fig. 5. Photoconductivity build-up after illumination with UV radiation power density of 250 mW/cm^2 (at 20 s) and decay after illumination removal (at 170 s) in a network of ZnO nanowires measured at room temperature (300 K) in ambient air at different applied bias (from top to bottom, the curves were obtained with an applied external bias of 5, 3, 1, –1, –3, and –5 V, respectively).

The fact that the shape of the relaxation curves is not affected by a change in the applied bias and the polarity of the bias indicates an insignificant influence of contact effects. The percolation of randomly oriented nanowires, as deduced from Fig. 1b, provides a pathway of current through the nanowire network, while the huge surface-to-volume ratio suggests the primordial importance of surface effects and that of oxygen molecules, since measurements are performed in ambient air. The photoresponse of ZnO in air is known to be governed by the adsorption (in the dark) and desorption (under UV illumination) of oxygen molecules [25]. In the dark, oxygen molecules adsorbed on the surface of ZnO nanowires capture free electrons of the *n*-type semiconductor: $O_2(g) + e^- \rightarrow O_2^-(ad)$. This produces a depletion layer near the nanowire surface, resulting in an upward band bending near the surface. Due to the large surface-to-volume ratio, the adsorption of O_2 significantly reduces the conductivity of the nanowires. UV-light illumination with a photon energy higher than E_g generates electron–hole pairs in the ZnO. Holes migrate to the surface along the potential slope created by the band bending and recombine with O_2-trapped electrons, thus releasing oxygen from the surface: $O_2^-(ad) + h+ \rightarrow O_2(g)$. The unpaired electrons are either collected at the anode or recombine with holes generated when oxygen molecules are readsorbed and ionized at the surface. Similar effects upon the PPC and optical quenching of PC from surface-induced carrier localization and strongly reduced recombination of holes with electrons trapped at the surface have been reported in GaN nanowires [24] and nanoperforated GaN membranes [31].

6. Conclusions

The results of this comparative study reveal a different nature of the transient PC in microgranular ZnO and ZnO nanowires prepared by oxidizing bulk ZnTe and ZnTe nanowires, respectively. The percolation of granules in microgranular ZnO provides a reliable current flow as in bulk materials, and the photoconductivity build-up and decay is determined by bulk defects including bulk charge carrier trapping centers, the PC relaxation time being on the order of tens or hundreds of milliseconds. The PC relaxation time in random networks of microwires is two orders of magnitude longer, being governed by surface states, SBB effects, and various adsorption–desorption processes, rather than by bulk trap effects. Most probably, oxygen molecules play a primordial role among these species.

References

[1] C. V. Reddy, A. Balakrishnan, H. Okumura, and S. Yoshida, Appl. Phys. Lett. 73, 244, (1998).
[2] C. Johnson, J. Y. Lin, H.X. Jiang, M. A. Khan, and C .J. Sun, Appl. Phys. Lett. 68, 1808, (1996).
[3] Z. Li, J.Y. Lin, H.X. Jiang, A Salvador, A. Botchkarev, and H. Morkoc, Appl. Phys. Lett. 69, 1474, (1996).
[4] D. V Lang and R. A. Logan, Phys. Rev. Lett. 39,635, (1977).
[5] D. V. Lang, R. A. Logan, and M. Jaros, Phys. Rev. B 19, 1015, (1979).
[6] J. Z. Li, J. Y. Lin, H. X. Jiang, M. A. Khan, and Q. Chen, J. Appl. Phys. 82, 1227, (1997).
[7] J.Z. Li, J.Y. Lin, H.X. Jiang, M.A. Khan, and Q. Chen, J. Vac. Sci. Technol. B15, 1117, (1997).
[8] J. Hubbard, Proc. R. Sot. London Ser. A 276,238, (1963).
[9] P. W. Anderson, Phys. Rev. Lett. 34, 953, (1975).
[10] G. D. Watkins, in Festkiirperpmbleme: Advances in Solid State Physics, edited by P. Grosse (Vieweg, Braunschweig, 1984), Vol. 24, 163 p.
[11] B. I. Shklovskii and A. L. Efros., JETP 60, 867, (1971); JETP 61, 816, (1971).
[12] M. K. Sheinkman and A. Ya. Shik, Fiz. Tekh. Poluprovodn. 10, 209 (1976) [Sov. Phys-Semicond. 10, 128 (1976)].
[13] R. R. Lowney and S. Mayo, J. Electr. Matter, vol. 21, p. 731, (1992).
[14] H. J. Queisser and D. E. Theodorou, Phys. Rev. B, vol. 33, p. 4027, (1986).
[15] V. S. Vavilov, P. C. Euthymiou, and G. E. Zardas, Phys.-Usp., vol. 42, p. 199, (1999).
[16] H. X. Jiang and J. Y. Lin, Phys. Rev. Lett. 64, 2547, (1990).
[17] H. X. Jiang and J. Y. Lin, Phys. Rev. B 40, 10025, (1989).
[18] J. Y. Lin and H. X. Jiang, Phys. Rev. B 41, 5178, (1990).
[19] H. X. Jiang, G. Brown, and J. Y. Lin, J. Appl. Phys. 69, 6701, (1991).
[20] V. Ursaki, I. M. Tiginyanu, P. C. Ricci, A. Anedda, S. Hubbard, and D. Pavlidis, J. Appl. Phys. 94, 3875, (2003).
[21] V. Popa, T. Braniste, M. A. Stevens-Kalceff, D. Gerthsen, P. Brenner, V. Postolache, V. Ursaki, and I. M. Tiginyanu, J. Nanoelectron. Optoelectron. 7, 730, (2012).
[22] M. V. Calin, V. V. Ursaki, I.M. Tiginyanu, L. Syrbu, V. P. Shontea, D. Esinenco, and S. Albu, Mold. J. Phys. Sci., vol.2, p. 62, (2003).

[23] V. Postolache, Proc. 2nd International Conference on Nanotechnologies and Biomedical Engineering, Chisinau, Republic of Moldova, April 18-20, (2013).
[24] H.-Y. Chen, R.-S. Chen, N. K. Rajan, F.-C. Chang, L.-C. Chen, K.-H. Chen, Y.-J. Yang, and M. A. Reed, Phys. Rev. B 84, 205443, (2011).
[25] C. Soci, A. Zhang, B. Xiang, S. A. Dayeh, D. P. R. Aplin, J. Park, X. Y. Bao, Y. H. Lo, and D. Wang, Nano Lett. 7, 1003 (2007).
[26] H. Kind, H. Yan, B. Messer, M. Law, and P. Yang, Adv. Mater. (Weinheim, Germany) 14, 158, (2002).
[27] Q. H. Li, Y. X. Liang, Q. Wan, and T. H. Wang, Appl. Phys. Lett. 85, 6389, (2004).
[28] S. Kumar., V. Gupta, and K. Sreenivas, Nanotechnology 16, 1167, (2005).
[29] D. Cammi and C. Ronning, Adv. Cond. Matter Phys. 2014, 184120, (2014).
[30] Ed. Monaico, V. Postolache, E. Borodin, V. V. Ursaki, O. Lupan, R. Adelung, K. Nielsch, and I. M. Tiginyanu, Semicond. Sci. Technol. 30, 035014, (2015).
[31] O. Volciuc, T. Braniste, I.Tiginyanu, M. A. Stevens-Kalceff, J.b Ebeling, T. Aschenbrenner, D. Hommel, V. Ursaki, and J. Gutowski, Appl. Phys. Lett. 103, 243113, (2013).
[32] V. Zalamai, A. Burlacu, V. Postolache, E.V. Rusu, V.V. Ursaki, and I.M. Tiginyanu, Mold. J. Phys. Sci. 9 (3–4), 308, (2010).
[33] M. Smirnov, A. P. Rambu, C. Baban, and Gh. I. Rusu, J. Adv. Res. Phys. 1, 021011, (2010).